Response of hydrological processes to land-cover and climate changes in Kejie watershed, south-west China

Xing Ma,[1,2] Jianchu Xu,[3]* Yi Luo,[4] Shiv Prasad Aggarwal[5] and Jiatong Li[6]

[1] *Kunming Institute of Botany, CAS, 132 Lanhei Road, Heilongtan, Kunming 650204, China*
[2] *Yunnan Institute of Environmental Science, 23 Wangjiaba, Qixiang Road, Kunming 650034, China*
[3] *World Agroforestry Centre-China Program, 132 Lanhei Road, Heilongtan, Kunming 650204, China*
[4] *Institute of Geographic Science and Natural Resource Research, CAS, Beijing 100101, China*
[5] *Indian Institute of Remote Sensing, NRSA, 4, Kalidas Road, Dehradun 248001, India*
[6] *Baoshan Hydrological Bureau, Longyang Road, Baoshan, 678000, China*

Abstract:

Land-cover/climate changes and their impacts on hydrological processes are of widespread concern and a great challenge to researchers and policy makers. Kejie Watershed in the Salween River Basin in Yunnan, south-west China, has been reforested extensively during the past two decades. In terms of climate change, there has been a marked increase in temperature. The impact of these changes on hydrological processes required investigation: hence, this paper assesses aspects of changes in land cover and climate. The response of hydrological processes to land-cover/climate changes was examined using the Soil and Water Assessment Tool (SWAT) and impacts of single factor, land-use/climate change on hydrological processes were differentiated. Land-cover maps revealed extensive reforestation at the expense of grassland, cropland, and barren land. A significant monotonic trend and noticeable changes had occurred in annual temperature over the long term. Long-term changes in annual rainfall and streamflow were weak; and changes in monthly rainfall (May, June, July, and September) were apparent. Hydrological simulations showed that the impact of climate change on surface water, baseflow, and streamflow was offset by the impact of land-cover change. Seasonal variation in streamflow was influenced by seasonal variation in rainfall. The earlier onset of monsoon and the variability of rainfall resulted in extreme monthly streamflow. Land-cover change played a dominant role in mean annual values; seasonal variation in surface water and streamflow was influenced mainly by seasonal variation in rainfall; and land-cover change played a regulating role in this. Surface water is more sensitive to land-cover change and climate change: an increase in surface water in September and May due to increased rainfall was offset by a decrease in surface water due to land-cover change. A decrease in baseflow caused by changes in rainfall and temperature was offset by an increase in baseflow due to land-cover change. Copyright © 2009 John Wiley & Sons, Ltd.

KEY WORDS   land-cover change; climate change; SWAT; hydrological processes; watershed

Received 2 March 2008; Accepted 6 November 2008

INTRODUCTION

Mountains have immense stores of fresh water and are critical to the coupled ocean-atmosphere and terrestrial system (Viviroli and Weingartner, 2002). They are the source of 30 to 60% of the fresh water available downstream in humid areas and 70 to 95% of the water available in semi-arid and arid environments (Messerli *et al.*, 2004). High mountain regions with extensive glacial and snow cover can provide good indications of climate change (Xu *et al.*, 2007a). Shrestha *et al.* (1999) and Liu and Chen (2000) suggest that warming in the Himalayas has been greater than the global average, indicating that high-altitude regions are among the most sensitive areas in terms of response to global climate change. Mountain environments are sensitive to human activities, particularly to land-cover changes (Bosch and Hewlett, 1982). Water resources and hydrological dynamics in river basins are altered by changes in climate and land

cover (Vorosmarty *et al.*, 2000; Wang *et al.*, 2007). Land-cover/climate changes are predicted to have important impacts on river flows and water resources from mountain regions. Given the complexity of hydro-meteorological processes in mountain watersheds, determining impacts of land-cover/climate changes on water sources is a challenge to researchers and policy makers. Important work has been carried out on the impact of climate change (Singh and Bengtsson, 2004) and changes in land cover (Fohrer *et al.*, 2005) on the hydrological dynamics of mountain watersheds. Changes in climate and land cover in the Himalayas are predicted to have severe, direct impacts on river flows, natural hazards, the ecosystem, and livelihoods and to have an impact on regional climate, namely, the strength and timing of the Asian monsoon (Xu *et al.*, 2007a).

Land-use practices and management of water resources are interdependent. Changes in land cover as a result of farming, grazing, logging and tree planting, and urbanization have affected the water balance and transformed the water-flow pathways in the terrestrial hydrological cycle (Chhabra *et al.*, 2006). The linear warming trend over the

---

100 years from 1906–2005 is 0·74 °C. There is a conviction that recent regional changes in temperature have had discernible impacts on physical and biological systems (IPCC, 2007). Recent studies show that climate change has altered water flows and resources in river basins (Chen *et al*., 2006; Rees and Collins, 2006). Current research into the effects of land-cover/climate changes on hydrological processes and water-related environmental services, and who are the winners and losers on different scales, is insufficient for formulation of useful policies (Calder, 2007; Noordwijk *et al*., 2004).

Nation states have a vested interest in the political and environmental security of the Himalayan region, or Asian 'water tower' (Xu *et al*., 2007b). Yunnan is a water conduit linking the Tibetan Plateau and the mainland of south-east Asia and China's coastal areas. During the past two decades, the Yangtze, Red, and Mekong rivers have flooded frequently. In China, both the state and Yunnan governments launched rigorous conservation efforts in the upper reaches of river basins to mitigate floods and secure environmental services (Weyerhaeuser *et al*., 2005). Two programmes, the Natural Forest Protection Programme (NFPP) and Sloping Land Conversion Programme (SLCP), were implemented following the floods in 1998. Population growth and economic development also brought dramatic changes in land cover to mountain watersheds in south-west China. The dramatic changes occurring in Kejie watershed led to its selection as a site for examination of the coupled impacts of land-cover/climate changes on hydrological processes.

This study attempts to identify changes in land cover and climate over the past half a century; simulate hydrological responses to them; and assess the impacts of such changes. The SWAT (Soil and Water Assessment Tool) was used in this study to examine the degree to which land-cover/climate changes affect hydrological processes.

MATERIAL AND METHODS

Description of the watershed

Kejie watershed, which is situated upstream on the Salween River, provides environmental goods and services to Baoshan Prefecture in Yunnan and downstream to Myanmar and Thailand. It is located in western Yunnan at a latitude of 24°46′06″N–25°22′39″N and longitude of 98°55′47″E–99°40′28″E and covers a total area of 1755 km² (Figure 1). Elevations range from 963 to 3076 masl. Donghe River, a major tributary of the Upper Salween, is the main water course and runs for 95·2 km with an average slope of 11° ranging from 1 to 88°. The valley includes Longyang City, one of the most productive farming areas in Yunnan, at elevations of less than 1700 m. Mountain terrain is dominant and elevations range from 2000 to 3000 m. The climate is sub-tropical in the valley
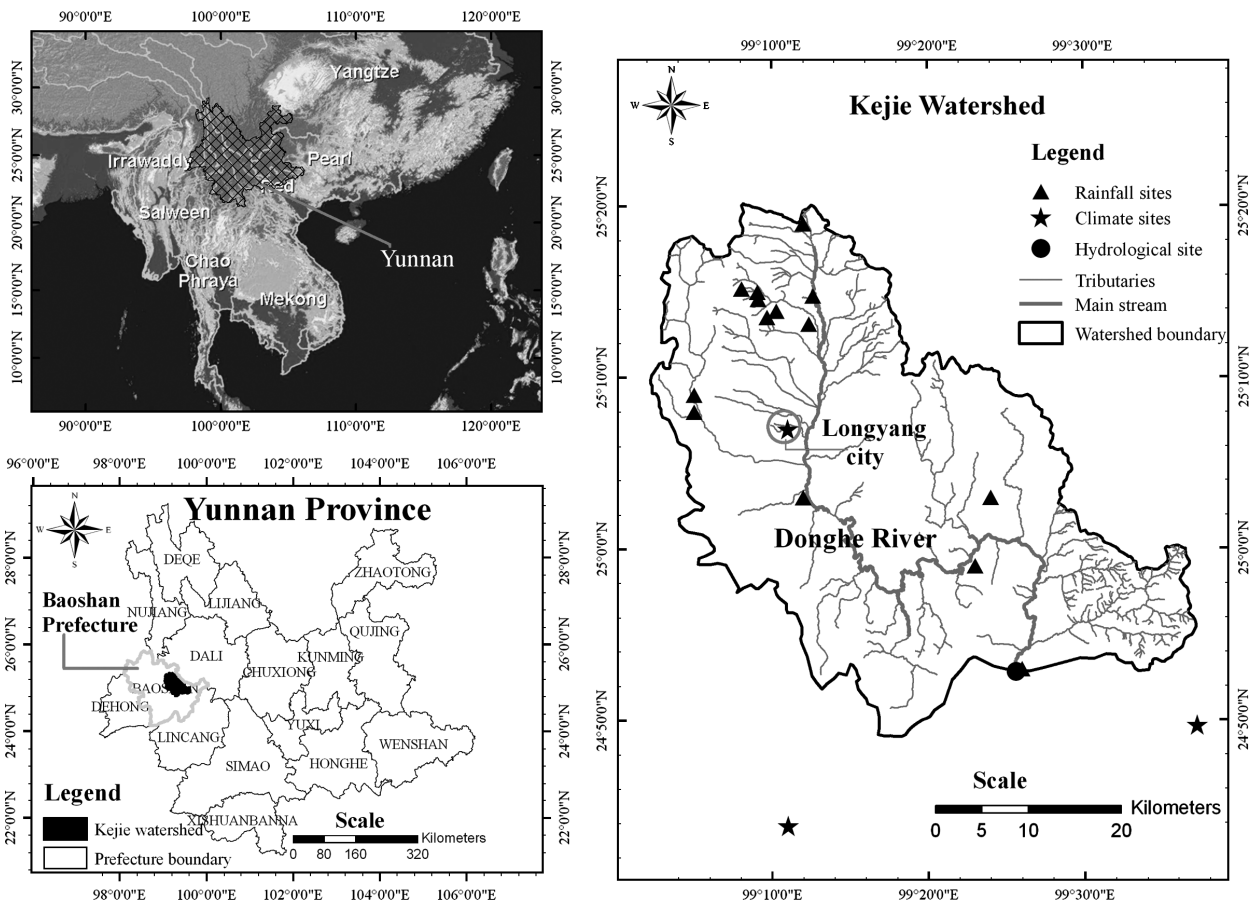

Figure 1. Location of Kejie watershed, China

and temperate in mountain areas. Annual precipitation varies between 970 and 1290 mm with an average of 966·5 mm. Dry and wet seasons are clearly defined. More than 80% of the precipitation occurs in the monsoon from May to October. The average temperature is 15·9 °C, the highest being 32·4 °C and the lowest −3·8 °C. The climate is influenced by the topography and temperatures decrease 0·6 °C with every 100 m of altitude. The main soil type is red soil. The natural vegetation of semi-moist broadleaved forest disappeared many decades ago and has been replaced by conifer with a mix of alder (*Alnus nepalensis*) and other broadleaved species.

There are 10 townships in Kejie watershed with a total population of 597 638 (2005). Longyang City is the political and economic centre of Baoshan Prefecture. Cropland predominates: two crops a year are planted, corn in summer and wheat or barley in winter for the uplands; and rice in the wet season and wheat in the dry season for the lowlands. The common cash crops are tea in the uplands, tobacco in the foothills, and vegetables in the lowlands. Natural forests were replaced by pine forests when shifting cultivation occurred in the 14th century. More recent causes of deforestation are (a) shifting cultivation, intensive planting of poppy and buckwheat, and overgrazing (early part of the twentieth century); (b) cutting trees for fuel for the army, housing, and road construction during World War II; (c) logging for fuel for iron and steel refining during the 'Great Leap Forward' in 1958; and (d) over-harvesting of forest resources following grants of individual household rights in the early 1980s (Xu et al., 2005; 2007b).

Description of land-cover changes

Several methods, based on satellite remote-sensing data, are used to describe patterns and processes of land-cover changes quantitatively. A transition matrix was used to explore the internal conversion of different land-cover types.

The percentage of 'conversion loss' or 'conversion gain' in relation to the total 'loss or gain' of a land-cover type was calculated according to the following formulae (Long et al., 2007).

$$P_{gain(i),j} = \frac{(a_{i,j} - a_{j,i})}{\left(\sum_{i=1}^{n} a_{i,j} - \sum_{j=1}^{n} a_{i,j}\right)} \times 100 \quad (1)$$

$$P_{loss(i),j} = \frac{(a_{j,i} - a_{i,j})}{\left(\sum_{i=1}^{n} a_{i,j} - \sum_{j=1}^{n} a_{i,j}\right)} \times 100 \quad (2)$$

where $P_{gain(i),j}$ is the percentage taken by land-cover type j (period $k + 1$) in the total 'conversion gain' of the type i (period k); $P_{loss(i),j}$ is the percentage taken by type j (period $k + 1$) in the total 'conversion loss' of type i (period k); $a_{i,j}$ denotes the area of land type i in period k converted to land type j in period $k + 1$; and $a_{j,i}$ denotes the area of land-cover type j in period k converted to land-cover type i in period $k + 1$.

Trend detection in hydrological time series

The Mann–Kendall (MK) test for monotonic trends and Mann–Whitney test for significant changes are used widely to detect monotonic trends and important changes (Yue et al., 2002; Xu et al., 2003, 2007; Partal and Kahya, 2006); and both of them were used in this study. The MK statistics are given as follows (Burn, 1994; Westmacott and Burn, 1997).

$$Z_c = \begin{cases} \dfrac{S - 1}{\sqrt{\text{var}(S)}}, & S > 0 \\ 0 & S = 0 \\ \dfrac{S + 1}{\sqrt{\text{var}(S)}}, & S < 0 \end{cases} \quad (3)$$

in which,

$$S = \sum_{i=1}^{n-1} \sum_{k=i+1}^{n} \text{sgn}(x_k - x_i) \quad (4)$$

where, x_k, x_i are the sequential data values, n is the length of the data set, and $\text{sgn}(\theta)$ is equal to 1, 0, −1 when θ is greater than, equal to, or less than zero, respectively. The null hypothesis H_0 (there is no trend) is accepted if $-Z_{1-\alpha/2} \le Z_c \le Z_{1-\alpha/2}$.

Given the data vector $X = (x_1, x_2, \ldots, x_n)$, partition X so that $Y = (x_1, x_2, \ldots, x_{n1})$ and $Z = (x_{n1+1}, x_{n2+2}, \ldots, x_{n1+n2})$. The Mann–Whitney equation is given as (Xu et al., 2003)

$$Z_c = \frac{\sum_{t=1}^{n_1} r(x_t) - n_1(n_1 + n_2 + 1)/2}{[n_1 n_2 (n_1 + n_2 + 1)/12]^{1/2}} \quad (5)$$

in which $r(x_t)$ is the rank of the observations. The null hypothesis H_0 (there is no steep change) is accepted if $-Z_{1-\alpha/2} \le Z_c \le Z_{1-\alpha/2}$.

Description of the watershed model

Hydrological modelling, especially distributed hydrological modelling, is used to simulate hydrological processes in watersheds. The objective of this study is to assess the effects of land-cover/climate changes on hydrological processes. The Soil and Water Assessment Tool (SWAT), which was designed to predict the impact of land management on water, sediment, and agricultural chemical yields over long periods of time in complex watersheds with different soil, land use, and management conditions, was used in this study because it has also been used successfully to model impacts of climate change on hydrological cycles in watersheds (Arnold et al., 1998) and to simulate impacts of land use on hydrological processes and distinguish the roles they played. The SWAT method has also been used on different varieties and sizes of watersheds (Arnold and Allen, 1996; Chu and Shirmohammadi, 2004; Arnold and Fohrer, 2005; Chaplot et al., 2005; Wu and Johnston, 2007).

The SWAT is based on the water balance in the soil profile and the processes simulated include precipitation, infiltration, surface runoff, evapotranspiration (ET), lateral flow, and percolation. The volume of surface runoff is predicted from daily rainfall by using the Soil Conservation Service (SCS) curve number method. The Muskingum method is used for channel water routing. For the present study, the Priestley and Taylor (1972) approach was selected to determine potential evapotranspiration. Actual evapotranspiration was determined using the methodology developed by Ritchie (1972). A description of all the components in SWAT can be found in the literature (Arnold and Allen, 1996; Arnold *et al*., 1998; Neitsch *et al*., 2004, 2005; Srinivasan *et al*., 1998).

Data preparation

Land use/cover and topography. Four satellite images, Landsat MSS (1974), Landsat TM (1991), Landsat ETM$^+$ (2001), and IRS P6 LISS 3 (2006), were used to interpret previous changes in land cover. The three Landsat images were downloaded from the Global Land Cover Facility's Earth Science Data Interface website; and the IRS P6 LISS 3 image, provided by the Centre for Space Science Technology Education in Asia and the Pacific (CSSTEAP), was purchased from the National Remote Sensing Agency (NRSA). Satellite images were processed in ERDAS Imagine 9·0 to identify categories of land cover based on spectral characteristics of the watershed using unsupervised classification and visual interpretation. Six land-cover domains were identified; namely, forest, grassland, cropland, settlement, barren land, and water. The image taken on 9 January 2006 was verified with 314 ground control points which were captured by GPS and covered all land-cover classes

A digital elevation model (DEM) of Kejie watershed with a spatial resolution of 50 m was derived from a contour map of the Kejie watershed. A drainage network map was digitized from topo-sheets of Baoshan Prefecture.

Hydro-meteorological data. There are three meteorological stations with long-term records, but two of these lie outside the watershed (Shidian and Changning) The Longyang station has long-term records and lies inside the watershed, and there is one other station in the watershed which has kept records for 5 years (Ganwangkeng). There are 12 rain gauges installed at elevations from 963 to 3076 m (Figure 1).

The Kejie Hydrological Station (KHS), which has kept daily discharge data for over 40 years, is located at the outlet of Kejie watershed. Daily outflow readings from a reservoir located on the upper reaches of the river have been collected since 1959 by Baoshan Department of Hydrology. Baseflow separation was carried out by the program of Arnold and Allen (1999) using the flow records kept by KHS from 1965 to 2005.

Hydrological and meteorological data were provided by the Baoshan Department of Hydrology and Meteorology. Hydrological data were cross-checked with upstream and downstream data and meteorological data scrutinized on a routine basis to process it for public use.

Soils: A soil map on a scale of 1 : 1 000 000 from the Nanjing Institute of Soil of the Chinese Academy of Sciences was used. The soil texture was of clay loam, loam, silty clay loam, and silty loam. Soil stratification; contents of sand, clay, and silt for soil layers; soil depths; soil organic matter; and maximum rooting depth were based on the soil survey report of Longyang Soil Department. Estimation of organic carbon content was based on soil organic matter and soil texture was calculated using the soil texture calculator found on the internet site http://soils.usda.gov/technical/aids/investigations/texture/. Bulk density and saturated hydraulic conductivity were estimated by using another soil calculator (http://www.nrel.colostate.edu/projects/century/) based on the percentages of clay, silt, and sand; and soil hydrological grouping was carried out according to soil texture and hydraulic conductivity. The study focused on water flow rather than on sediment loss, so the soil erodibility factor used in SWAT simulations was taken from the SWAT soil database.

Vegetation/crop parameters. Monsoon evergreen broadleaved forest is the dominant vegetation type in the study area: it is rich in *Castanopsis sp., Schima sp, C. hystrix, C. indica, S. wallichii, Pinus kesiya var. langbianensis, and P. yunnanensis*. The vertical spatial distribution of vegetation is deciduous monsoon forest and open shrubs in the dry-hot valley (<1100 m); monsoon evergreen broadleaved forest (1000–1700 m) and montane moist evergreen broadleaved forest (1600–2500 m); coniferous and broadleaved mixed forest (2300–2900 m); moss evergreen coppice (2800–3000 m); and coniferous forest (>3000 m) (Wu and Zhu, 1987). The land-cover types used in the model were forest, grassland, cropland, settlement, barren land, and water. The land-cover and plant growth parameters used were from the SWAT default database since no measurements or publications were available.

Delineation of sub-watersheds and derivation of homogeneous hydrological response units (HRUs). Delineation of the basin into sub-basins was carried out automatically with a threshold area of 3200 ha based on the digital elevation model (DEM): consequently, the watershed was divided into 31 sub-basins. Land-cover and soil maps were overlaid to generate HRUs for each sub-basin. Accordingly, 262 and 267 HRUs were drawn with threshold values of 10% for soils and 5% for land cover in 1974 and 2001, respectively.

A reservoir is connected to sub-basin No 2 and the watershed has one outlet situated near the Kejie Hydrological Station.

Model calibration and validation

Monthly flow records from 1971–1979 were split into two segments, 1971–1975 and 1976–1979, in order to

calibrate and validate parameters. Calibration was carried out manually through trial and error until satisfactory results were obtained. Parameters used for calibration included CN2 (Curve Number); GWQMN (threshold depth of water required in a shallow aquifer for return flow to occur); Alpha_BF (baseflow alpha factor); SOL_K (saturated hydraulic conductivity); SOL_AWC (available water capacity of soil layers); and ESCO (soil evaporation compensation factor) because these were the most suitable for measuring water flow by sensitivity analysis in the watershed. The performance of the calibrated parameters was evaluated by graphic comparison and statistical indices—Nash–Sutcliff efficiency (NSE), percentage bias (PBIAS), and ratio of the root mean square error to the standard deviation of measured data (RSR).

NSE, PBIAS, and RSR were used to evaluate the modelling (Moriasi *et al.*, 2007). NSE indicates how well the plot of observed versus simulated data fits the 1 : 1 line: the performance is perfect if NSE = 1. PBIAS measures the average tendency of the simulated data to be larger or smaller than their observed counterparts: the optimal value of PBIAS is 0·0, with low-magnitude values indicating accurate model simulation. RSR standardizes root mean square error (RMSE) using the observed standard deviation: the lower RSR is, the better the performance of the model simulation. The equations for NSE, PBIAS, and RSR are as follows.

$$NSE = 1 - \left[\frac{\sum_{i=1}^{n}(Y_i^{obs} - Y_i^{sim})^2}{\sum (Y_i^{obs} - Y^{mean})^2} \right] \quad (6)$$

$$PBIAS = \left[\frac{\sum_{i=1}^{n}(Y_i^{obs} - Y_i^{sim}) \times (100)}{\sum_{i=1}^{n} Y_i^{obs}} \right] \quad (7)$$

$$RSR = \frac{RMSE}{STDEV_{obs}} = \frac{\sqrt{\sum_{i=1}^{n}(Y_i^{obs} - Y_i^{sim})^2}}{\sqrt{\sum_{i=1}^{n}(Y_i^{obs} - Y^{mean})^2}} \quad (8)$$

where Y_i^{obs} is the ith observation for the constituent being evaluated, Y_i^{sim} is the ith simulated value for the constituent being evaluated, Y^{mean} is the mean of the observed data for the constituent being evaluated, and n is the total number of observations.

Differentiated impact of land-cover and climate changes

To differentiate between the impacts of land-cover/climate changes on hydrological processes, simulations were carried out for two different periods (1965–1986 and 1987–2005). Land-cover maps for 1974 and 2001 were used to present land-cover conditions for the two periods. Four simulations: namely, a combination of the land-cover map for 1974 with the climate data for 1965–1986 (simulation 1), the land-cover map for 2001 with the climate data for 1965–1986 (simulation 2), the land-cover map for 1974 with the climate data for 1987–2005 (simulation 3), and the land-cover map for 2001 with the climate data for 1987–2005 (simulation 4) were carried out using the SWAT model. Simulations 1 and 4 attempted to depict what had happened in the watershed in the two periods. Simulation 2 was to depict the impacts of land-cover change on hydrological processes by assuming there was no climate change from periods 1 to 2. Finally, simulation 3 attempted to reveal the impacts of climate change on hydrological processes by assuming there was no land-cover change from periods 1 to 2. The results of simulations 1 and 4 were compared with the measured mean annual streamflow from periods 1 and 2. The relative error of the measured and simulated values was within 15%, which indicated that the simulations were acceptable. The difference between the results of simulations 3 and 1 gave an indication of the effect of climate change on hydrological processes, and the difference between the results of simulations 2 and 1 indicated the impact of land-cover change on hydrological processes.

RESULTS AND DISCUSSIONS

Land-cover changes

The overall accuracy of land-cover classification is about 72·6% and the overall Kappa statistics 0·67. Land-cover maps for 1974, 1991, 2001, and 2006 are given in Figure 2. The areas of land under different cover types and their changes are given in Table I and illustrated in Figure 3. Comparing the land-cover maps for 1974 and 2006, the land-cover changes can be summarized as increases in forest cover by 22·4% (accounting for the total area of the watershed) and settlement by 2·5%; and decreases in grassland cover by 15·4%, cropland by 6·7%, barren land by 2·6% and water bodies by 0·2%.

The intersection method in ERDAS Imagine 9·0 and four land-cover maps (Figure 2) were used to generate the conversion matrices of land-use changes. The net change and internal change (conversion loss or conversion gain) were calculated on the basis of the matrices using formulae (1) and (2) (Table II).

From 1974 to 1991, the area under forest increased by 219·2 km², 54·9% of which was gained from grassland, 24·5% from cropland, and 18·3% from barren land; barren land decreased by 101·1 km², 43·9% of which had become converted forest and 42·9% cropland; grassland decreased by 63·3 km², 193·4% of which was caused by reforestation, although 85·8% was gained from cropland; cropland area decreased by 60·1 km², 91·8% of which was caused by conversion to forest, 91·0% by conversion to grassland, and 73·4% was gained from barren land; the settlement area increased by 3·3 km², 262·7% and 25·7% of which was gained from barren land and grassland, whereas 107·3 and 87·2% had been converted to forest
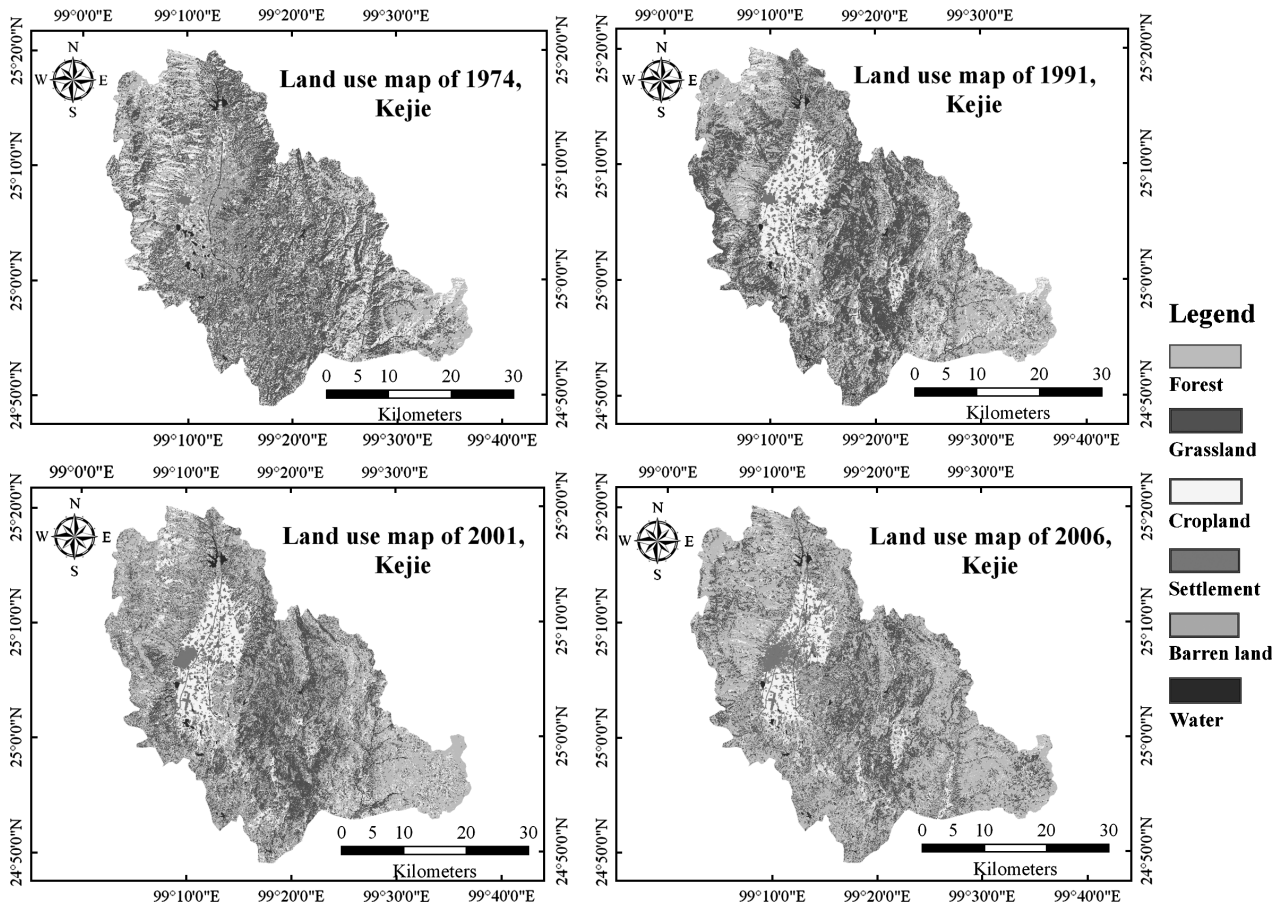
Figure 2. Land-cover maps of Kejie watershed (1974–2006), China

Table I. Statistics for land-cover areas and changes in Kejie watershed (1974–2006) on the basis of satellite images (km^2)

Land use	1974	1991	2001	2006	1974–1991	1991–2001	2001–2006
F	385·4	604·6	654·7	778·3	+219·2	+50·1	+123·6
G	493·7	430·4	298·4	223·4	−63·3	−132·0	−75·0
C	475·4	415·3	455·6	357·8	−60·1	+40·3	−97·8
S	57·3	60·6	73·2	101·4	+3·3	+12·6	+28·2
BL	331·4	230·3	257·5	285·4	−101·1	+27·2	+27·9
W	14·8	13·4	15·2	10·4	−1·4	+1·8	−4·8

F = forest; G = grassland; C = cropland; S = settlement; BL = barren land; W = Water. '+' indicates an increase and '−' indicates a decrease.
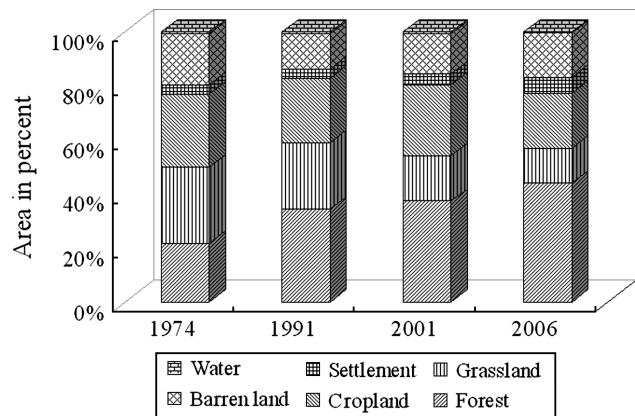

Figure 3. Land-cover change in Kejie watershed (1974–2006), China

and cropland, respectively; water bodies decreased by 1·4 km^2, 192 and 96% of which had been converted to forest and cropland, whereas 165·2 and 38·7% had been gained from barren land and grassland, respectively.

From 1991 to 2001, forest increased by 50·1 km^2, 119·7% of which was gained from grassland; grassland decreased by 132 km^2 and 45·5, 39, and 15·5% of it had been converted to forest, barren land, and cropland, respectively; cropland increased by 40·3 km^2, 64·1 and 50·7% of which was gained from barren land and grassland, respectively, and 12·8% of which had been converted to settlement respectively; settlement increased by 12·6 km^2, 41·2, 31, and 22·3% of which had been gained

from cropland, barren land, and forest respectively; barren land increased by 27·2 km^2, 188·9 and 22·5% of which was gained from grassland and forest and 94·9 and 14·3% had been converted to cropland and settlement respectively; water bodies increased by 1·8 km^2, 109·5 and 35·1% of which was from forest and barren land and 47·3% had been converted to settlement.

From 2001 to 2006, forest increased by 123·6 km^2, 44·8% of which was gained from cropland, 33·6% from grassland, and 20·1% from barren land; grassland decreased by 75 km^2, 54·7% of which had been converted to forest, 38·2% to barren land, and 5·8% to

Table II. Internal conversion rates between land-cover classes for different periods in Kejie watershed

Land-cover classes		1991 land-cover change (%)					
		F	G	C	S	BL	W
1974	F	0	−193·4	−91·8	−107·3	−40·0	−96·0
	G	+54·9	0	−91·0	+25·7	−6·1	+38·7
	C	+24·5	+85·8	0	−87·2	−42·9	−192·0
	S	+1·7	−1·4	+5·0	0	−8·9	−15·9
	BL	+18·3	+9·8	+73·4	+262·7	0	+165·2
	W	+0·6	−0·8	+4·3	+6·2	−2·2	0

		2001 land-cover change (%)					
		F	G	C	S	BL	W
1991	F	0	−45·5	−2·2	+22·3	+22·5	+109·5
	G	+119·7	0	+50·7	−0·9	+188·9	+9·0
	C	+1·8	−15·5	0	+41·2	−94·9	−6·3
	S	−5·6	+0·1	−12·8	0	−14·3	−47·3
	BL	−12·2	−39·0	+64·1	+31·0	0	+35·1
	W	−3·8	−0·1	−0·8	+6·5	−2·2	0

		2006 land-cover change (%)					
		F	G	C	S	BL	W
2001	F	0	−54·7	−55·7	+0·7	−88·6	−42·4
	G	+33·6	0	+0·6	+15·6	+103·6	+7·5
	C	+44·8	+0·8	0	+52·8	+109·4	−24·1
	S	−0·2	−5·8	−15·2	0	−28·6	−16·6
	BL	+20·1	−38·2	−30·9	+28·1	0	−24·4
	W	+1·7	−0·5	+1·1	+2·8	+4·2	0

'+' indicates a conversion gain and '−'indicates a conversion loss.

settlement; cropland decreased by 97·8 km², 55·7% of which had been converted to forest, 30·9% to barren land, and 15·2% to settlement; settlement increased by 28·2 km², 52·8% of which was gained from cropland, 28·1% from barren land, and 15·6% from grassland; barren land increased by 27·9 km², 103·6% of which was gained from grassland and 109·4% from cropland, whereas 88·6% had been converted to forest and 28·6% to settlement; water bodies decreased by 4·8 km², 42·4% of which had been converted to forest, 24·4% to barren land, 24·1% to cropland, and 16·6% to settlement.

In general, from 1974–1991, the trend was conversion of grassland to forest, cropland to forest and grassland, and barren land to forest and cropland; from 1991–2001, the predominant trend was conversion of grassland to forest, barren land and cropland, and barren land to cropland; from 2001–2006, the obvious trend was conversion of grassland to forest and barren land, of cropland to forest, barren land and settlement, and of barren land to forest.

The trends derived from satellite data were consistent with the statistics from Longyang Department of Forestry. The changes were mainly caused by the government reforestation policy in 1987 which led to an increase in forest and decreases in grassland, cropland, and barren land. Settlements and cropland also increased from 1991 to 2001 when the population increased.

Changes in temperature, rainfall, and streamflow

Trend analysis was carried out for the annual temperature, rainfall at Longyang meteorological station, and annual streamflow at Kejie hydrological station (the outlet of the watershed). The results of the Mann–Kendall time series' test on monotonic trends for annual temperature, rainfall, and streamflow are summarized in Table III. The results show that the null hypothesis H_0 was rejected by the annual temperature time series, and H_0 was not rejected by the time series for annual rainfall and streamflow. In other words, the long-term monotonic trend in annual temperature is statistically significant, whereas the long-term monotonic trend in annual rainfall and streamflow is weak over time and statistically insignificant.

A five-year moving average analysis was carried out for annual average air temperature, runoff, and rainfall (Figure 4). An inflection point (in 1986) was identified through visual observation, and this coincides with the Tarim River Basin in north-west China (Chen *et al.*, 2006). The annual temperature of two meteorological stations in Yunnan Province (Tengchong Station 180 km away from Longyang Station and Kunming Station about 580 km away from Longyang Station) were tested to show the trend in temperature change in Baoshan. An inflection point (1986) was identified for the two other stations (Figure 5). The inflection point divided the data series for temperature, rainfall, and streamflow into two periods: 1 (1965–1986) and 2 (1987–2005). The Mann–Whitney test was applied and the test results are listed in Table III. The results show that there is a significant change in annual temperature between periods 1 and 2. Statistics for the annual temperature, rainfall, and streamflow for different periods are listed in Table IV. Between periods 2 and 1, the mean values of annual temperature, rainfall, and streamflow increased by 0·9 °C, 9·7 mm, and 22·1 mm, respectively.

The Mann–Kendal test and Mann–Whitney test were applied to data series for monthly rainfall and temperature. The results showed that the monthly temperatures in January, March, and April had a noticeable monotonic trend and significant change. There was a

Table III. Monotonic trend test and significant change test for annual rainfall, temperature and streamflow time series in Kejie watershed

	Mann–Kendall test		Mann–Whitney test			
	Z_c	H_0[a]	n_1	n_2	Z_c	H_0[b]
Rainfall	0·461	A	22	19	−0·13	A
Temperature	5·403	R	22	19	−5·03	R
Streamflow	−0·303	A	22	19	−0·55	A

[a] H_0 is the hypothesis that there is no monotonic trend in the time series for annual rainfall, temperature, and streamflow.
[b] H_0 is the hypothesis that there is no significant change in the time series for annual rainfall, temperature, and streamflow.
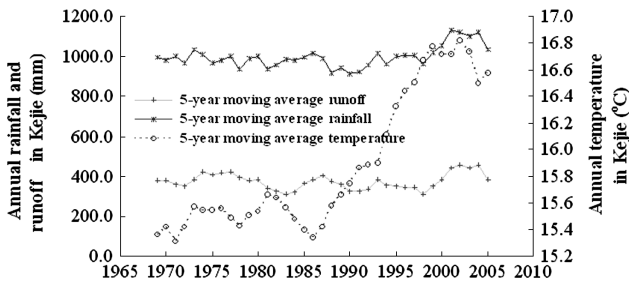A = Accepted; R = Rejected. Significance level $\alpha = 0.05$.

Figure 4. 5-years moving average rainfall, runoff and air temperature in Kejie watershed (1965–2005), China
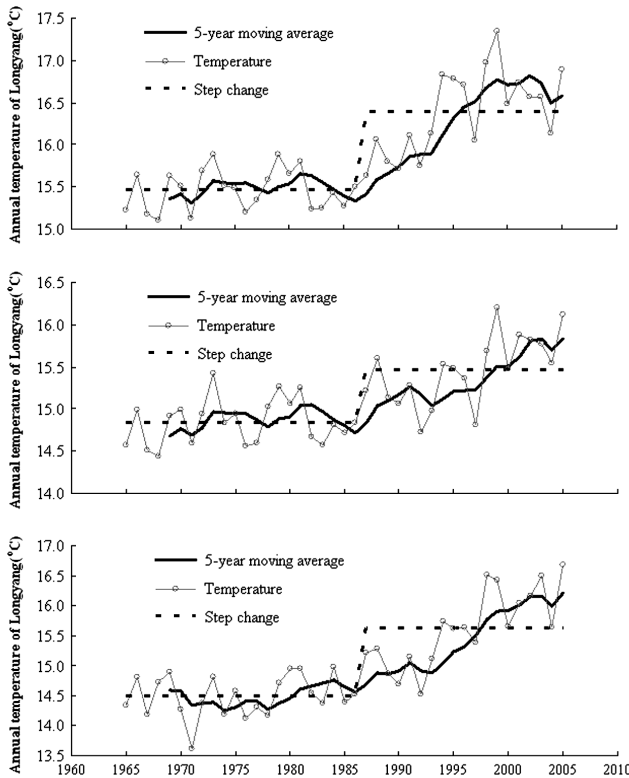

Figure 5. Change trend in annual temperature in Longyang, Tengchong and Kunming Stations in Yunnan Province (1965–2005), China

statistically significant monotonic trend and noticeable change in monthly rainfall in September. The changes in monthly rainfall in May, June, and July were more obvious (Table V). There were changes in the mean monthly temperature and rainfall from periods 1 to 2 (Figure 6) and the amplitude of increased temperature was 0·8 °C

higher in the dry season (from November to April) than in the wet season (from May to October). The monthly rainfall increased by 54·9 and 43·1% in September and May and decreased by 27·6 and 14·4% in June and July respectively. The increase in rainfall in May indicated the earlier onset of the monsoon, and the change in monthly rainfall from May to September indicated the variability of the monsoon. A comparison of monthly average streamflow between periods 1 and 2 showed increases in May, September, and October and decreases in June, July, and August: no statistically significant trend was found.

'Revisiting' hydrological history using model simulation

An increase in temperature may result in an increase in atmospheric water vapour, melting of snow and ice, increasing evaporation, and changes in soil moisture and runoff. Dettinger *et al.* (2004) found that mountain snowpack melted earlier after an increase in temperature in California, and the results of Stewart *et al.* (2004) showed that increasing temperatures in North America caused earlier occurrences of spring runoff. The simulation results of Singh and Bengtsson (2004) showed that increasing temperatures caused decreases in streamflow in winter, summer, and autumn; however, streamflow increased in spring in western Himalayan rivers. Chen *et al.* (2006) reported significant and subtle increasing trends and slight decreasing trends in streamflow at different headwaters of the Tarim River when temperature and precipitation increased.

Impacts of land-cover change on hydrological processes are variable for different places. Streamflow increased due to reforestation in the upper-stream area of the Yangtze River (Cheng, 1991), whereas it increased following deforestation in the Loess Plateau area (Liu and Zhong, 1978) of China. Streamflow decreased under forested areas (Van Lill *et al.*, 1980; Bosch and Hewlett, 1982; Scott and Smith, 1997; Legesse *et al.*, 2003); and this is a new finding in terms of the effect of forestation on streamflow (Calder, 2005). Sandstroem (1995) and Elkaduwa and Sakthivadivel (1998) indicated that baseflow increased following reforestation; whereas Smith and Scott (1992) and Loerup and Hansen (1997) indicated that baseflow decreased following reforestation.

This study found that annual streamflow decreased by 22·1 mm with an increase in temperature (0·9 °C) and

Table IV. Statistics for annual rainfall, temperature, and streamflow for different periods in Kejie watershed

Variables	Rainfall (mm)		Temperature (°C)		Streamflow (mm)	
Periods	1	2	1	2	1	2
Time Series	1965–1986	1987–2005	1965–1986	1987–2005	1965–1986	1987–2005
Length of Record	22	19	22	19	22	19
Mean value	994·4	1004·0	15·5	16·4	387·4	365·3
Max value	1290·1	1368·3	15·9	17·4	567·0	636·1
Min value	767·4	729·3	15·1	15·6	240·6	189·3
Standard Deviation	134·73	174·16	0·25	0·51	94·74	117·97
Coefficient of variation	0·14	0·17	0·02	0·03	0·24	0·32

Table V. Monotonic trend test and significant change test for monthly rainfall time series in Kejie watershed

Monthly rainfall	Mann–Kendall test		Mann-Whitney test			
	Z_c	$H_0{}^a$	n_1	n_2	Z_c	$H_0{}^b$
January	−0·382	A	22	19	−0·065	A
February	0·056	A	22	19	−0·405	A
March	−0·640	A	22	19	−0·131	A
April	−0·865	A	22	19	−1·620	A
May	1·471	A	22	19	−1·673	A
June	−0·887	A	22	19	−1·672	A
July	−1·775	A	22	19	−1·294	A
August	−0·348	A	22	19	−0·261	A
September	2·370	R	22	19	−2·275	R
October	−0·202	A	22	19	−0·327	A
November	0·067	A	22	19	−0·222	A
December	0·461	A	22	19	−0·275	A

[a] H_0 is the hypothesis that there is no monotonic trend in the time series for monthly rainfall.
[b] H_0 is the hypothesis that there is no significant change in the time series for monthly rainfall.
A = Accepted; R = Rejected. Significance level $\alpha = 0.05$
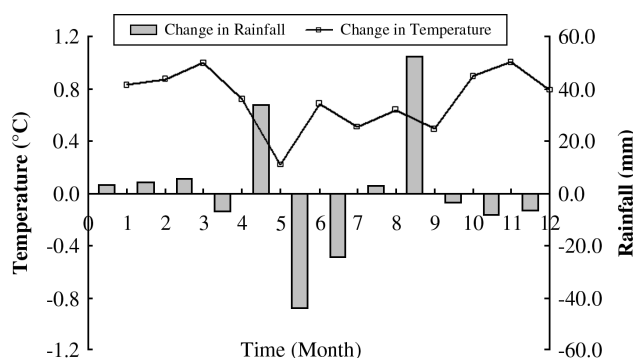

Figure 6. Change variation of mean monthly temperature and rainfall between period 1 (1965–1986) and period 2 (1987–2005) in Kejie watershed, China

rainfall (9·7 mm) combined with reforestation (69% of forest area in 1974) in the study area. The decrease in observed annual streamflow may be attributed to the effect of reforestation offset by the increase caused by climate change, or a decrease caused by reforestation and climate change, or a decrease caused by climate change offset by an increase with reforestation. How and to what degree changes in land cover/and climate affect hydrological components (namely, surface water, baseflow, evapotranspiration, lateral flow, and streamflow) remain to be investigated.

Model calibration and validation. The parameters of alpha 0·028 and a groundwater delay time of 80 days were obtained. The results also showed that baseflow contributed 54% of the total flow, which was close to the 48% found by Xu (1996).

The calibration and validation results are given in Figure 7, with NSE = 0·75, RSR = 0·50, and PBIAS = −2·3% for calibration and NSE = 0·91, RSR = 0·30, and PBIAS = −5·3% for validation, indicating that performance of the model ranged from good to very good in line with the general performance ratings of Moriasi *et al.* (2007). The calibration model parameters were thus accepted for the scenario simulations.

Differentiated impact of land-cover/climate changes on hydrological processes. Table VI shows the simulated streamflow and the change in streamflow due to land-cover/climate changes. Impacts of land-cover/climate changes on hydrological processes are summarized in Table VII. In terms of the joint impacts of land-cover/climate changes, from periods 1 to 2 the mean annual surface water decreased by less than 15% and the streamflow decreased and baseflow and actual ET increased by less than 5%.

In terms of land-cover change, the major change was an increase in forest cover at the expense of grassland, cropland, and barren land. Reforestation resulted in a decrease in mean annual surface water (26·7 mm) and streamflow (15·8 mm) and an increase in mean annual evapotranspiration (15·9 mm) and baseflow (12·9 mm) in Kejie watershed. Reforestation may result in a decrease in annual discharge (Guo *et al.*, 2008; Hu *et al.*, 2004).
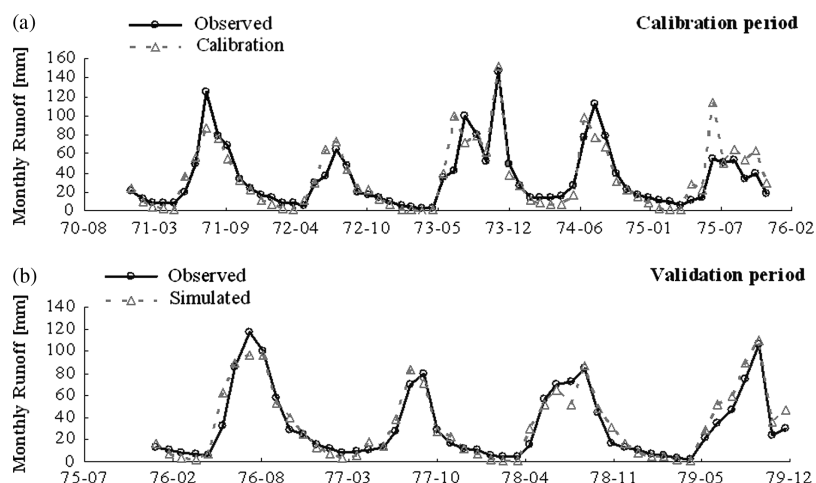

Figure 7. Mean monthly simulated and observed runoff at the outlet of Kejie watershed for (a) the calibration period and (b) the validation period

Table VI. Contribution of land-cover and climate changes to streamflow changes between periods 1 and 2 in Kejie watershed

Simulation				Changes from simulated results					
			Simulated stream flow	Caused by combined factor (Sim4-Sim1)		Caused by climate change (Sim3-Sim1)		Caused by land cover (Sim2-Sim1)	
			mm	mm	%	mm	%	mm	%
Sim 1	CLD	65–86	425·6						
	LCM	74							
Sim 2	CLD	65–86	409·8						
	LCM	2001							
Sim 3	CLD	87–05	430·0	−11·5	−2·7	4·4	1·0	−15·8	−3·7
	LCM	74							
Sim 4	CLD	87–05	414·1						
	LCM	2001							

CLD = Climate data; LCM = Land-cover map.

Table VII. Effects of land-cover/climate changes on hydrological processes in Kejie watershed

Hydrological processes	Change		Land-cover contribution		Climate contribution		Difference	
	mm	%	mm	%	Mm	%	mm	%
Surface water	−16·6	−11·1	−26·7	−17·8	11·5	7·7	−1·4	−1·0
Baseflow	5·6	3·4	12·9	7·8	−7·2	−5·0	1·0	0·6
Lateral flow	−0·7	0·0	−2·1	−1·9	1·0	0·9	0·4	1·0
Actual ET	21·7	4·9	15·9	3·6	5·8	1·3	0·0	0·0
Streamflow	−11·5	−2·7	−15·8	−3·7	4·4	1·0	−0·1	0·0

This may be because forest vegetation intercepts and loses more water through evapotranspiration than other land-cover types and, hence, reduces surface water volume and streamflow. Bruijnzeel (1990) indicated that the infiltration properties of the forest are critical in determining how the water available is partitioned between runoff and recharge. In Kejie watershed, an increase in forest caused increased baseflow; and this could be because of increased infiltration into soil profiles.

Climate change caused an increase of 11·5 mm in surface water; 4·4 mm in streamflow; 5·8mm in actual ET; and a decrease of 7·2mm in baseflow. The increase in surface water and streamflow may be mostly due to the increase in rainfall. The increased ET could be a result of increased temperature and rainfall. The decrease in baseflow could be due to the fact that the recharge of groundwater decreases when evapotranspiration increases; and this is in turn affected by the seasonal variation of rainfall in the study area.

In terms of monthly distribution of the effects of land-cover change on hydrological processes from periods 1 to 2 (Figure 8), 90% of the decrease in surface water was concentrated in the wet season. Baseflow increased about 4 and 9 mm in the dry and wet season respectively. In the dry season, the increase in baseflow played an important role in the ecosystem; 92% of the actual ET occurred in the wet season; and streamflow decreased by 16·9 mm from April to November and increased by 1·2 mm in December, January, February, and March.

In terms of monthly distribution of the effects of climate change on hydrological processes from periods 1 to 2 (Figure 8), surface water increased in May and September due to a significant increase in rainfall in those two months; and decreased in June and July due to a decrease in rainfall and an increase in temperature in the same period. Baseflow increased by 1·3 mm in the dry season and decreased by 8·5 mm in the wet season: baseflow was determined by the infiltration rate and soil moisture storage capacity. A decrease in rainfall in June reduced the antecedent water content of the soil in July resulting in a decrease in baseflow. The decrease in rainfall in July continued to reduce baseflow in August. The baseflow began to rise from September with an increase in rainfall in August. The actual ET increased in May, mainly due to the high temperature and heavy rainfall. Streamflow decreased by 21·6 mm in June, July, November, and December and increased by 26·0 mm in the remaining months.

The monthly distribution of effects of coupled land-cover and climate change on hydrological processes from periods 1 to 2 illustrated the seasonal variation of hydrological components (Figure 9). The pattern of change in hydrological processes was mainly determined by the changes in climate. An increase in monthly surface water caused by climate change was offset by a decrease caused by changes in land cover. A decreased baseflow caused by variations in rainfall was offset by increased baseflow due to reforestation. Streamflow decreased in June and July and increased in May and September. The
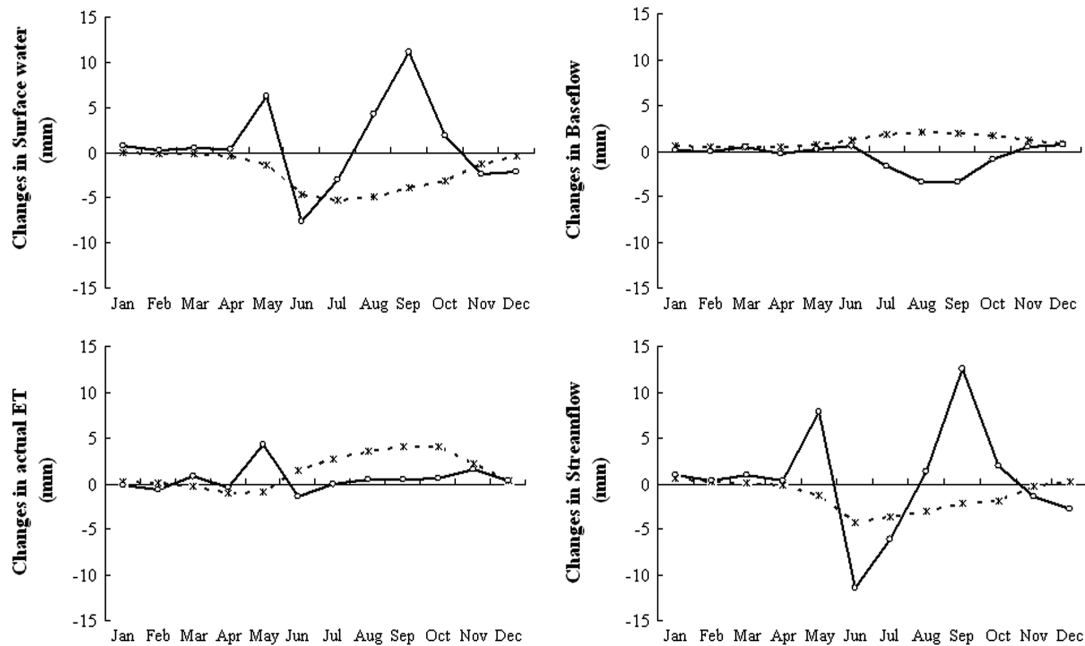
Figure 8. Monthly changes in surface water, actual ET, baseflow and streamflow over the period 1 and period 2 under land-cover/climate change in Kejie watershed, China. Solid line describes the effects of climate change, and broken line describes the effects of land-cover change
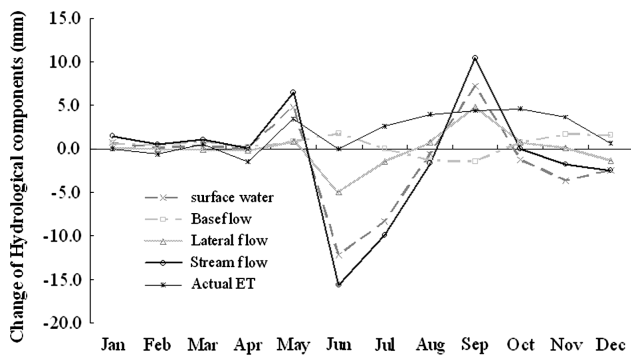

Figure 9. Monthly changes of hydrological components over period 1 and period 2 under coupled land-cover/climate change in Kejie watershed

changes in surface water and lateral flow patterns were similar to streamflow; and streamflow coincided with monthly changes in rainfall (Figures 6 and 9).

The comparative annual and seasonal effects of land-cover/climate changes on hydrological processes in the past four decades are as follows.

1. Land-cover change played a dominant role in mean annual values.
2. Seasonal variations in surface water and streamflow were mainly influenced by seasonal variations in rainfall, and changes in land-cover played a regulating role in this respect.
3. Surface water was more sensitive to land-cover/climate changes and the increase in surface water in September and May due to the increase in rainfall was offset by a decrease in surface water due to land-cover change.
4. The decrease in baseflow caused by changes in rainfall and temperature was compensated for by the increase in baseflow due to land-cover change.

CONCLUSION

On the basis of historical hydro-meteorological data combined with satellite images, we cross-checked to triangulate the interaction of hydro-meteorological effects and land. The SWAT was applied to simulate different combinations of land-cover/climate changes. The main conclusions were as follows.

In the past four decades, land-cover changes have occurred in the Kejie watershed. The major changes were increases in forest area (22·4%) at the expense of grassland (15·4%), cropland (6·7%), and barren land (2·6%) along with an increase in settlement (2·5%). A noticeable monotonic trend has occurred in the annual temperature pattern in the past four decades, and a significant change occurred around 1986 in the study area: mean annual temperature increased from 15·5 °C to 16·4 °C. The long-term monotonic trend in annual rainfall and streamflow was weak, whereas the changes in monthly rainfall in May, June, July, and September were obvious.

Reforestation in the study area led to an increase in evapotranspiration and baseflow and decreases in surface water and streamflow, especially in the wet season (from May to October). Surface water is more sensitive to land-cover change than other hydrological components.

Climate change in the study area led to increases in surface water, evapotranspiration, and streamflow and to decreases in baseflow. Monthly changes were influenced mainly by the variability of rainfall. An increase in temperature combined with variable rainfall caused variations in streamflow and surface water over the year.

The differentiated impacts of land-cover/climate changes on hydrological processes revealed that the unapparent change in streamflow is implicitly because the

effects of land-cover change on hydrological processes were offset by the effects of climate change, and the effects of climate change were offset by the variability of rainfall. Land-cover changes in the past four decades have played an important role in hydrological processes in the study area and have contributed to the mitigation of negative impacts caused by climate change.

REFERENCES

Arnold JG, Allen PM. 1996. Estimating hydrological budgets for three Illinois watersheds. *Journal of Hydrology* **176**: 55–77. DOI: 10·1016/0022-1694(95)02782-3.

Arnold JG, Allen PM. 1999. Automated methods for estimating baseflow and groundwater recharge from streamflow records. *Journal of the American Water Resources Association* **35**: 411–424. DOI:10·1111/j.1752-1688.1999.tb03599.x.

Arnold JG, Srinivasan P, Muttiah RS, Williams JR. 1998. Large area hydrological modeling and assessment—Part I: Model development. *Journal of the American Water Resources Association* **34**: 73–89. DOI:10·1111/j.1752-1688.1998.tb05961.x.

Arnold JG, Fohrer N. 2005. SWAT2000: current capabilities and research opportunities in applied watershed modeling. *Hydrological Processes* **19**: 563–572. DOI: 10·1002/hyp.5611.

Bosch JM, Hewlett JD. 1982. A review of catchment experiments to determine the effect of vegetation changes on water yield and evapotranspiration. *Journal of Hydrology* **55**: 3–23. DOI: 10·1016/0022-1694(82)90117-2.

Bruijnzeel LA. 1990. *Hydrology of Moist Tropical Forests and Effects of Conversion: A State of Knowledge Review*. UNESCO International Hydrological Programme: Paris.

Burn DB. 1994. Hydrologic effects of climate change in west central Canada. *Journal of Hydrology* **160**: 53–70.

Calder IR. 2005. *Blue Revolution—Integrated Land and Water Resource Management*. London and VA: Earthscan and Sterling Publications: London and VA.

Calder IR. 2007. Forest and water-ensuring forest benefits outweigh water costs. *Forest Ecology and Management* **251**: 110–120. DOI: 10·1016/j.foreco.2007·06·015.

Chaplot V, Saleh A, Jaynes DB. 2005. Effect of accuracy of spatial rainfall information on the modeling of water, sediment, and NO3-N loads at the watershed level. *Journal of Hydrology* **312**: 223–234. DOI: 10·1016/j.jhydrol.2005·02·019.

Cheng GW. 1991. An approach to the relationship between runoff characters and forest in the basin of Sichuan. *Journal of Soil and Water Conservation* **5**: 48–52 (Chinese). cnki: ISSN: 1009–2242·0·1991-01-006.

Chen YN, Takeuchi K, Xu Ch, Chen YP, Xu ZX. 2006. Regional climate change and its effects on river runoff in the Tarim Basin, China. *Hydrological Processes* **20**: 2207–2216. DOI: 10·1002/hyp.6200.

Chhabra A, Geist H, Houghton RA, Haberl H, Braimoh AK, Vlek P, Patz J, Xu JC, Ramankutty N, Coomes O, Lambin EF. 2006. Multiple impacts of land use/cover change. In *Land-use and Land-cover Change: Local Processes and Global Impacts*, Lambin EF, Geist HJ (eds). Springer: Berlin: 71–116.

Chu TW, Shirmohammadi A. 2004. Evaluation of the SWAT model's hydrology component in the Piedmont physiographic region of Maryland. *Transactions of the ASAE* **47**: 1057–1073.

Dettinger M, Cayan D, Meyer M, Jeton A. 2004. Simulated hydrologic responses to climate variations and changes in the Merced, Carson, and American river basins, Sierra Nevada, California, 1900–2099. *Climate Change* **62**: 283–317.

Elkaduwa WKB, Sakthivadivel R. 1998. Use of historical data as a decision support tool in watershed mangament: a case study of the Upper Nilwala basin in Sri Lanka. Research Report 26. Colombo, Sri Lanka: International Water Management Institute.

Fohrer N, Haverkamp S, Frede HG. 2005. Assessment of the effects of land use patterns on hydrological landscape functions: development of sustainable land use concepts for low mountain range areas. *Hydrological Processes* **19**: 659–672. DOI: 10·1002/hyp.5623.

Guo H, Hu Q, Jiang T. 2008. Annual and seasonal streamflow response to climate and land-cover changes in the Poyang Lake basin, China. *Journal of Hydrology* **355**: 106–122. DOI: 10·1016/j.jhydrol.2008·03·020.

Hu Q, Wilson GD, Chen X, Akyuz A. 2004. Effects of climate and land cover change on stream discharge in the Ozark highlands, USA. *Environmental Modelling & Assessment* **10**: 9–19.

IPCC. 2007. Climate change 2007: synthesis report. Contribution of working groups I, II and III to the Fourth Assessment Report of the Intergovernmental Panel on Climate Change [Core writing team, Pachauri PK and Reisinger A]. IPCC, Geneva.

Legesse D, Vallet-Coulumb C, Gasse F. 2003. Hydrological response of a catchment to climate and land use changes in tropical Africa: case study south central Ethiopia. *Journal of Hydrology* **275**: 65–85. DOI: 10·1016/S0022-1694(03)00019-2.

Liu CM, Zhong JX. 1978. A preliminary study to relationship between forest and annual runoff in loess plateau. *Acta Geographica Sinica* **33**: 112–126 (in Chinese).

Liu XD, Chen BD. 2000. Climatic warming in the Tibetan Plateau during recent decades. *International Journal of Climatology* **20**: 1729–1742. DOI: 10·1002/1097-0088(20001130)20 : 14<1729::AID-JOC556>3·0.CO;2-Y.

Loerup JK, Hansen E. 1997. Effect of land use on the streamflow in the southwestern highlands of Tanzania. In *Sustainability of Water Resources under Increasing Uncertainty*, Rosbjerg D, Boutayeb N, Gustand A, Kundzewicz ZW, Rasmussen PF (eds), *IAHS Publication No.* 240. IAHS Press: Wallingford; 227–236.

Long HL, Tang GP, Li XB, Heilig GK. 2007. Socio-economic driving forces of land-use change in Kunshan, the Yangtze River Delta economic area of China [J]. *Journal of Environmental Management* **83**: 351–364. DOI:10·1016/j.jenvman.2006·04·003.

Messerli B, Viviroli D, Weingartner R. 2004. Mountains of the world: vulnerable water towers for the 21st century. *Ambio* **13**: 29–34.

Moriasi DN, Arnold JG, Van Liew MW, Bingner RL, Harmel RD, Veith TL. 2007. Model evaluation guidelines for systematic quantification of accuracy in watershed simulations. *Transactions of the ASABE* **50**: 885–900.

Neitsch SL, Arnold JG, Kiniry JR, Srinivasan RS, Williams JR. 2004. Soil and water assessment tool input/output file documentation, version 2005. http://www.brc.tamus.edu/swat/downloads/doc/swat2005/SWAT%202005%20io.pdf. [last access 23 Dec. 2007].

Neitsch SL, Arnold JG, Kiniry JR, Williams JR. 2005. Soil and water assessment tool: theoretical documentation, version 2005. http://www.brc.tamus.edu/swat/downloads/doc/swat2005/SWAT%202005%20theory%20final.pdf. [last access 23 Dec. 2007].

Noordwijk MV, Poulsen JG, Ericksen PJ. 2004. Quantifying off-site effects of land use change: Filters, flows and fallacies. *Agriculture, Ecosystems and Environment* **104**: 19–34. DOI: 10·1016/j.agee.2004·01·004.

Partal T, Kahya E. 2006. Trend analysis in Turkish precipitation data. *Hydrological Processes* **20**: 2011–2026. DOI: 10·1002/hyp.5993.

Priestley CHB, Taylor RJ. 1972. On the assessment of surface heat flux and evaporation using large-scale parameters. *Monthly Weather Review* **100**: 81–92. DOI: 10·1175/1520-0493(1972)100<0081:OTAOSH>2·3.CO;2.

Rees GH, Collins DN. 2006. Regional differences in response of flow in glacier-fed Himalayan rivers to climate warming. *Hydrological Processes* **20**: 2157–2169. DOI: 10·1002/hyp.6206.

Ritchie JT. 1972. A model for predicting evaporation from a row crop with incomplete cover. *Water Resources Research* **8**: 1204–1213.

Sandstroem K. 1995. Forests and Water- Friends or Foes: Hydrological implication of deforestation and land degradation in semi-arid Tanzania. In *Linkoeping Studies in Arts and Science* 120. Department Theme Research, Sweden: University of Linkoeping.

Scott DF, Smith RE. 1997. Preliminary empirical models to predict reduction in total and low flows resulting from afforestation. *Water SA* **23**: 135–140.

Shrestha AB, Wake CP, Mayewski PA, Dibb JE. 1999. Maximum temperature trends in the Himalaya and its vicinity: An analysis based on temperature records from Nepal for the period 1971-94. *Journal of Climate* **12**: 2775–2787. DOI: 10·1175/1520-0442(1999)012<2775:MTTITH>2·0.CO;2.

Singh P, Bengtsson L. 2004. Hydrological sensitivity of a large Himalayan basin to climate change. *Hydrological Processes* **18**: 2363–2385. DOI:10·1002/hyp.1468.

Smith RE, Scott DF. 1992. The effects of afforestation on low flows in various regions of South Africa. *Water SA* **18**: 185–194.

Srinivasan R, Ramanarayanan TS, Arnold JG, Bednarz ST. 1998. Large area hydrological modeling and assessment part II: model application. *Journal of American Water Resource Association* **34**: 91–101. DOI:10·1111/j.1752-1688·1998.tb05962.x.

Stewart I, Cayan D, Dettinger M. 2004. Changes in snowmelt runoff timing in western North America under a "Business as Usual" climate change scenario. *Climate Change* **62**: 217–232.

Van Lill WS, Kruger FJ, Van Wyk DB. 1980. The effects of afforestation with *Eucalyptus grandis* Hill EX Maiden and *Pinus patula* Schlecht. Et Chan. On streamflow from experimental catchments at Mokobulaan, Transvaal. *Journal of Hydrology* **48**: 107–118.

Viviroli D, Weingartner R. 2002. The significance of mountains as sources of the world's freshwater. *GAIA-Ecological Perspectives for Science and Society* **11**(3): 182–186.

Vorosmarty CJ, Green P, Salisbury J, Lammers RB. 2000. Global water resources: vulnerability from climate change and population growth. *Science* **289**: 284–288. DOI: 10·1126/science.289·5477·284.

Wang GX, Liu JQ, Kubota J, Chen L. 2007. Effect of land-use changes on hydrological processes in the middle basin of the Heihe River, northwest China. *Hydrological Processes* **21**: 1370–1382. DOI: 10·1002/hyp.6308.

Westmacott JR, Burn DH. 1997. Climate changes effects on the hydrologic regime within the Churchill-Nelson river basin. *Journal of Hydrology* **202**: 263–279.

Weyerhaeuser H, Wilkes A, Kahrl F. 2005. Local impacts and responses to regional forest conservation and rehabilitation programs in China's northwest Yunnan province. *Agricultural Systems* **85**: 234–253. DOI:10.1016/j.agsy.2005·06·008.

Wu KSH, Johnston CA. 2007. Hydrological response to climatic variability in a Great Lakes watershed: A case study with the SWAT model. *Journal of Hydrology* **337**: 187–199. DOI: 10·1016/j.jhydrol.2007·01·030.

Wu ZY, Zhu YC. 1987. *Yunnan Vegetation* [M]. Science Press: Beijing (in Chinese).

Xu CJ. 1996. Theory and methods on estimation of baseflow in higher land, Yunnan. *Water Resources Research* **17**: 11–22 (in Chinese).

Xu JC, Ai XH, Deng XQ. 2005. Exploring the spatial and temporal dynamics of land use in Xizhuang Watershed of Yunnan, southwest China. *International Journal of Applied Earth Observation and Geoinformation* **7**: 299–309.

Xu JC, Shrestha AB, Vaidya R, Eriksson M, Hewitt K. 2007a. The melting Himalayas: Regional challenges and local impacts of climate change on mountain ecosystems and livelihoods, ICIMOD technical paper, Kathmandu.

Xu JC, Yang YP, Fox J, Yang XF. 2007b. Forest transition, its causes and environmental consequences: empirical evidence from Yunnan of Southwest China. *Tropical Ecology* **48**(2): 137–150.

Xu ZX, Takeuchi K, Ishidaira H. 2003. Monotonic trend and step [sic] changes in Japanese precipitation. *Journal of Hydrology* **279**: 144–150. DOI: 10·1016/S0022-1694(03)00178-1.

Xu ZX, Li JY, Liu CM. 2007. Long-term trend analysis for major climate variables in the Yellow river basin. *Hydrological Processes* **21**: 1935–1948. DOI:1·1002/hyp.6405.

Yue S, Pilon P, Cavadias G. 2002. Power of the Mann-Kendall and Spearman's rho test for detecting monotonic trends in hydrological series. *Journal of Hydrology* **259**: 254–271.